



ORIGINAL ARTICLE

Learning, memory and blood–brain barrier pathology in Duchenne muscular dystrophy mice lacking Dp427, or Dp427 and Dp140

Minou Verhaeg¹  | Kevin Adamzek¹ | Davy van de Vijver¹ | Kayleigh Putker¹ | Sarah Engelbeen¹ | Daphne Wijnbergen¹ | Maurice Overzier¹ | Ernst Suidgeest² | Louise van der Weerd^{1,2} | Annemieke Aartsma-Rus¹ | Maaïke van Putten¹ 

¹Department of Human Genetics, Leiden University Medical Center, Leiden, The Netherlands

²C.J. Gorter MRI Center, Department of Radiology, Leiden University Medical Center, Leiden, The Netherlands

Correspondence

Maaïke van Putten, Department of Human Genetics, Leiden University Medical Center, Leiden, The Netherlands.

Email: m.van_putten@lumc.nl

Funding information

Duchenne Parent Project-NL, Grant/Award Number: 15.003; Duchenne Parent Project Belgium

Abstract

Duchenne muscular dystrophy is a severe neuromuscular disorder that is caused by mutations in the *DMD* gene, resulting in a disruption of dystrophin production. Next to dystrophin expression in the muscle, different isoforms of the protein are also expressed in the brain and lack of these isoforms leads to cognitive and behavioral deficits in patients. It remains unclear how the loss of the shorter dystrophin isoform Dp140 affects these processes. Using a variety of behavioral tests, we found that *mdx* and *mdx*^{4cv} mice (which lack Dp427 or Dp427 + Dp140, respectively) exhibit similar deficits in working memory, movement patterns and blood–brain barrier integrity. Neither model showed deficits in spatial learning and memory, learning flexibility, anxiety or spontaneous behavior, nor did we observe differences in aquaporin 4 and glial fibrillary acidic protein. These results indicate that in contrast to Dp427, Dp140 does not play a crucial role in processes of learning, memory and spontaneous behavior.

KEYWORDS

cognition, dystrophin, neuromuscular disease, spatial learning, spontaneous behavior

1 | INTRODUCTION

Duchenne muscular dystrophy (DMD) is a recessive X-linked neuromuscular disorder affecting approximately 1 in 5000 newborn males.¹ It is characterized by progressive muscle weakness, eventually leading to premature death in the third or fourth decade of a patient's life due to respiratory and/or cardiac failure.² In addition to the musculature's pathological hallmarks, a significant proportion of DMD patients also presents with cognitive impairments from an early age onwards. The

overall intelligence quotient of DMD patients is one standard deviation below the population mean^{3,4} and approximately 30% of DMD patients suffer from neuronal disorders or behavioral problems,⁵ including autism spectrum disorder, attention-deficit hyperactivity disorder, inattention, reading deficits, obsessive-compulsive disorder, anxiety, depression and epilepsy.^{3,6–9}

DMD is caused by mutations in the *DMD* gene, which prevent synthesis of functional dystrophin protein. The *DMD* gene is the largest known human gene and contains 7 unique promoter regions,

This is an open access article under the terms of the [Creative Commons Attribution-NonCommercial-NoDerivs](https://creativecommons.org/licenses/by-nc-nd/4.0/) License, which permits use and distribution in any medium, provided the original work is properly cited, the use is non-commercial and no modifications or adaptations are made.

© 2024 The Authors. *Genes, Brain and Behavior* published by International Behavioural and Neural Genetics Society and John Wiley & Sons Ltd.

which give rise to different dystrophin isoforms that are expressed in a tissue and/or cell-specific manner. Only the full-length isoform Dp427m (427 kDa, muscle) is expressed in muscle, whereas five dystrophin isoforms are expressed in the central nervous system (CNS). The full-length isoform Dp427c is predominantly expressed in neurons of the cortex and CA regions of the hippocampus,^{10,11} while Dp427p is expressed in the cerebellar Purkinje cells.¹² The shorter isoform Dp140 is expressed in the cerebral cortex in fetal life stages and in the cerebellum postnatally.¹³ Dp71 and Dp40 are ubiquitously expressed at high levels throughout the CNS.¹³ The role of the different dystrophin isoforms in the CNS is only partly understood. Dp427 has been suggested to be involved in synapse structure and functioning.¹⁴ Dp140 seems to play a role in pre-synaptic plasticity in the excitatory synapses.¹⁵ Dp71 is associated with blood-brain barrier (BBB) permeability¹⁶ and synaptic organization,¹⁷ while Dp40 plays a possible role in presynaptic function.¹⁸

Depending on the location of the mutation, DMD patients lack one or multiple dystrophin isoforms, that is, DMD patients with a mutation in the 5' end of the *DMD* gene only lack the Dp427 isoforms, while those with a mutation in the 3' end of the *DMD* gene either lack Dp427 and Dp140 or all dystrophin isoforms in the CNS. A correlation between the amount of missing isoforms and the severity and incidence of cognitive deficits seems to exist.^{8,19,20} However, it is still unclear how the lack of the distinct dystrophin isoforms in the CNS affects cognition, behavior and overall brain pathology.

The consequences of dystrophinopathy on behavior and brain pathology have been studied in several DMD mouse models. *Mdx* mice, which have a point mutation in exon 23 and consequently lack Dp427, have been most thoroughly studied. They show impaired functioning in cognitive processes concerning social behavior,²¹ spatial and recognition memory,²² depressive-like behavior²³ and anxiety and fear.^{24–26} Only recently, the consequences of the additional lack of Dp140 have been investigated in the *mdx52* mouse, which have a deletion of exon 52, and *mdx^{4cv}* mice, which have a nonsense mutation in exon 53. Both mouse models show deficits in cognitive processes such as fear and social behavior.^{27–29} However, direct comparisons between mice lacking only Dp427 and mice lacking Dp427 + Dp140 are minimal, making it difficult to understand the exact effects of the lack of Dp140.

To further investigate the consequences of the lack of one or multiple dystrophin isoforms in more detail, we subjected *mdx* and *mdx^{4cv}* mice to behavioral tests and MRI analyses. In working memory related tasks we observed an equally decreased performance in *mdx* and *mdx^{4cv}* mice, while only *mdx* mice showed a delay in spatial learning. *Mdx* and *mdx^{4cv}* mice both displayed increased performance in a food related task and affected movement patterns during spontaneous behavior. No differences were found in memory flexibility or anxiety. Furthermore, *mdx* and *mdx^{4cv}* mice showed similar increases in BBB permeability. Overall, the lack of Dp140 did not seem to have additional effects on different types of memory, spontaneous behavior or BBB function in mice.

2 | MATERIALS AND METHODS

2.1 | Mice

Male *mdx* (*mdx*(BL6) $n = 25$),³⁰ *mdx^{4cv}* (B6Ros.Cg-*Dmd^{mdx-4cv}*/J $n = 23$)³¹ and wild type (WT) mice (C57BL/6J $n = 21$), were bred at the animal facility of the Leiden University Medical Center (LUMC). Heterozygous females of each of the DMD strains were paired with WT males to generate DMD and WT males from the same litters. WT mice were taken equally from litters of both strains for experiments, and since no statistical differences were observed between the two, we considered them as one WT group. Mice were housed in individually ventilated cages (Makrolon type II), filled with sawdust and enriched with cardboard nesting material, with 12 h dark/light cycles. Mice had ad libitum access to water and standard RM3 chow (SDS, Essex, United Kingdom). Experiments were performed at the animal facility of the LUMC in rooms dedicated for behavioral experiments. The experiments were approved by the Central Authority for Scientific Procedures on Animals and conform with the Directive 2010/63/EU of the European Parliament.

2.2 | Behavioral tests

2.2.1 | Experimental setup

Starting between 10 and 15 weeks of age, mice were subjected to a series of experiments spread over a 5 week period. The experiments consisted of the T-maze, Morris water maze (MWM), and housing in a PhenoTyper automatic home cage for 7 days in which spontaneous behavior, anxiety and discrimination and reversal learning were assessed (Figure 1). All experiments were performed at the same time of the day. Spontaneous behavior was automatically tracked in the PhenoTyper cages 24 h a day. Animal behavior and location were tracked with Ethovision XT, at a rate of 20 frames per second.

2.2.2 | T-maze

After 2 days of handling, a T-maze (white PVC, arms $30 \times 10 \times 25$ cm) was used to assess spatial working memory of the mice. During the learning trial, mice were released in the start arm and given 60 s to enter one of the goal arms. A door was lowered upon entering the goal arm and the mouse was maintained there for 30 s before it was removed from the maze. The test trial was performed directly after the learning trial. Here, the mouse was contained in the start location for 10 s after which it was allowed to walk through the maze for 60 s. In total, six learning and test trials were executed over a period of 2 days, with at least 1 h rest in between tests. Four *mdx* and four *mdx^{4cv}* mice were excluded because they did not complete the trials.

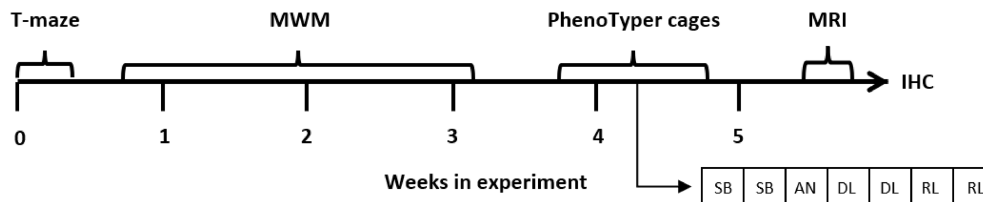


FIGURE 1 Overview of the experimental setup. Mice started between 10 and 15 weeks of age and underwent testing via T-maze, Morris water maze (MWM), PhenoTyper cages and a series of MRI scans. AN, anxiety; DL, discrimination learning; RL, reversal learning; SB, spontaneous behavior.

2.2.3 | Morris water maze

The MWM was used to assess the spatial- and reversal learning. The MWM consists of a circular pool (diameter = 120 cm) filled with dyed, non-transparent water. The maze contains a platform (diameter = 11 cm) located just below the surface of the water, half way between the center of the pool and the wall. Three distinct distal cues located outside the maze allowed mice to navigate through the pool. The test protocol consisted of an acquisition- and reversal learning phase. The acquisition trials, in which mice learned to locate the hidden platform, were conducted over a period of 5 days, with four trials per day. Hereto, the platform was located in the north-west quadrant of the pool and starting positions of mice were semi-randomly allocated according to the strategy in Vorhees et al.³² If the animal failed to locate the platform within 2 min, it was placed onto the platform, where it was allowed to stay for 15 s before being taken out. Three days after the last acquisition phase, a probe trial was performed, during which the platform was removed and swimming behavior was monitored for 2 min.

In the reversal learning phase, the platform was relocated in the south-east quadrant and swimming behavior was recorded for 2 min, or until the platform was reached. Trials were performed in a similar manner as in the acquisition phase, but included 4 days instead of five, after which a probe trial was conducted.

2.2.4 | PhenoTyper automated home-cages

A PhenoTyper automated home-cage (Noldus PhenoTyper 3000, Noldus Information Technology), with transparent Perspex walls (30 × 30 × 35 cm) and opaque Perspex floor, was used to assess the mice's behavior. The home-cage included sawdust bedding and was equipped with a drinking and feeding station. A rectangular shelter (10 × 10 × 5 cm) with two entrances (diameter 3 cm) was fixed in one corner. An infrared camera was mounted in the top.

2.2.5 | Spontaneous behavior

Mice were put into the automated home-cages during the light phase (5–9 h after the start of the light phase) with ad libitum access to water and standard RM3 chow. Mice were individually housed and

the location of the mice (middle of the body) was continuously tracked for 48 h, starting from the first dark phase. Twenty parameters for spontaneous behavior were calculated from the automatic tracked location of the mice and analyzed as described by Loos et al. for the dark and light phase of day 2.³³ Since automatic tracking was successful for all the mice, no manual scoring was necessary. Due to the 24 h tracking system of the PhenoTyper cages, the exact same time windows could be used for all the mice. Furthermore, total distance and velocity were analyzed as an indicator for muscle function. Two *mdx* mice and one *mdx*^{4cv} mouse were excluded from analyses due to a technical issue with their recordings. We did not have to exclude mice based on their sleeping behavior, since none of them slept outside their shelter (exclusion criteria of Loos et al.³³).

2.2.6 | Anxiety test

An anxiety test was conducted to examine the behavioral response of the mice to an external trigger, that is, a bright light-emitting diode (LED) spot.³⁴ A bright LED light (700 lux) was automatically activated for the duration of 1 h, 75 min after the start of the third dark phase (20.15 h local time at the animal facility). The LED light was positioned between the feeding station and the left shelter entrance. Time spent outside the shelter was calculated per block of 15 min for a duration of 2 h and 15 min (20.00 till 22.15 local time at animal facility). Two *mdx* mice and one *mdx*^{4cv} mouse were excluded from analyses due to a technical issue with their recordings.

2.2.7 | Discrimination and reversal learning task

On the fourth day, ad libitum standard chow was removed and an opaque Perspex wall with three entrances (17 cm wide, 25 cm high, 3 cm diameter holes) was placed in front of a pellet dispenser tube which protruded through the corner opposite of the shelter.³⁵ Water was accessible ad libitum during the entire behavioral trial. During the two-day discrimination learning phase, the mice received one food pellet (Dustless Precision Pellets, 14 mg, Rodent Purified diet, Bio Serv, Frenchtown, NJ, USA) after five entries through the left hole of the cognition wall, which did not have to be consecutive. Directly thereafter, 2 days of reversal learning were initiated in which the target hole changed from the left to the right hole.

Discrimination and reversal learning was defined as the total number of entries needed to reach a 80% criterion of correct entries. This was calculated via a moving window of 30 entries.

After completion of the trials, mice were transferred back to individually ventilated cages with ad libitum access to water and standard RM3 chow. Mice were housed individually for the remainder of the study.

2.3 | Magnetic resonance imaging analyses

MRI scans were generated from 10 randomly selected mice per strain using a 7T Bruker PharmaScan system (Bruker Biospin, Ettlingen, Germany). Mice were anesthetized with isoflurane (4% induction and 1.5% maintenance) after which an intraperitoneal canula was placed. Thereafter, mice were fixed onto the bed with ear bars and a tooth-bar, and an RF-coil was placed over the head of the mice. A water-heated thermos-coupled pad placed underneath the mice was used to control the body temperature with a rectal probe. Throughout the MRI scans, respiratory rate and body temperature were monitored.

MRI scans included a localizer scan and a T2-weighted Turbo RARE scan to determine volumes of the total brain and brain regions (echo time 39 ms, repetition time 2345.121 ms, averages 12, repetition 1, echo spacing 13 ms, RARE factor 8, slice thickness 0.7 mm, 19 slices, image size 250 × 208 mm, field of view 18 × 15 mm). Dynamic contrast-enhanced MRI (DCE-MRI) was done using T1-weighted RARE scans to determine BBB integrity (echo time 13.2 ms, repetition time 700 ms, averages 8, repetition 1, echo spacing 6.6 ms, RARE factor 4, slice thickness 0.5 mm, 19 slices, image size 196 × 196 mm, field-of-view 18 × 15 mm). After the first T1W RARE scan, the protocol was interrupted and mice were injected with 100 µL of contrast solution (ProHance Gadoteridol, Bracco diagnostics Inc., NJ, USA-produced by BIPSO, Singen, Germany), through the intraperitoneal canula before resuming the remaining six T1W RARE scans acquired over 42 min. To determine regions of interest, data was segmented using an atlas with 23 brain regions.^{36–39} Data acquisition, image reconstruction and visualization were performed with Paravision 6.0.1. software (Bruker Biospin Ettlingen, Germany). The time course of the signal intensity changes was used for statistical analyses.

2.4 | Sectioning and aquaporin 4 staining

After the MRI scans, mice were sacrificed by CO₂ without recovery from anesthesia. The brain was isolated and immediately frozen by covering it with dry ice powder. All samples were stored at –80°C. Coronally oriented sections (12 µm thick) were generated with a cryostat and stored at –80°C. Before staining, slides were washed with 0.1 M phosphate-buffered saline (PBS) and blocked with a mixture of 5% goat serum (Sigma-Aldrich, cat no. G9023-10ML) and 0.1% Triton X-100 (sigma-Aldrich cat. No. T9284-500ML) for 1 h. Tissue sections were incubated with primary antibody (anti-aquaporin 4, Sigma-Aldrich, AB3594-50UL, diluted 1:500 and anti-GFAP,

ThermoFisher, 13-0300, 1:250, diluted in PBS with 0.1% Triton and 1% goat serum) overnight. Sections were washed and incubated with secondary antibody (donkey anti-rabbit, ThermoFisher, A-21207 and donkey anti-rat, ThermoFisher, A-21208, both 1:250, diluted in PBS with 0.1% Triton and 1% goat serum) for 45 min and cover slipped with ProLong Gold mounting medium with DAPI (Invitrogen, cat. No. P36931). Images were made with a Zeiss AxioScan slide scanner at a 20 times magnification. Three sections per mouse were stained and scanned and one optimal section was selected via visual inspection, based on similarity in location within the brain, and minimal freezing damage or interference from other artifacts. Fluorescence images were converted into gray scales and intensities were determined in the cortex and hippocampus regions on one image per mouse using mean gray value in ImageJ. Analyses were done on one hemisphere. The ROI in the cortex was located close to the longitudinal fissure (Figure 7). For each image, data was then normalized against background levels, which were determined per image at 3 locations within the original ROI to account for difference in intensity caused by the imaging.

2.5 | Data analysis

All data were checked for normality and equal variance. See Table S1 for an overview of the tests per parameter. *F*- and *t*-values corresponding to significant *p*-values can be found in Table S2.

In case of normality and equal variance, group differences were determined by Tukey HSD tests. Comparisons with chance levels were made via a one sample *t*-test per group. If normality and equal variance was not met, Kruskal–Wallis tests were performed and if significant, additional Mann–Whitney repeated tests were performed. Comparisons to chance levels were made with a one-sample Wilcoxon signed-rank test per group.

Linear mixed models were used to assess time and strain differences for acquisition and reversal learning in the MWM and to assess for strain and time differences in baseline and in anxiety condition in the anxiety test in the PhenoTypers. These analyses were performed in Rstudio (version 4.3.1) using the LmerTest package (version 3.1.3).

Discrimination- and reversal learning in the PhenoTypers was tested with the Martel–Cox test.

Multiple comparison corrections were applied to the parameters of spontaneous behavior and the MRI scans using false discovery rate (FDR).

All data is presented as mean ± standard error of the mean (SEM).

p* < 0.05, *p* < 0.01, ****p* < 0.001.

3 | RESULTS

3.1 | DMD mice show decreased but not fully impaired performance in a working memory task

To assess spatial working memory, spontaneous alternation was measured with the T-maze (Figure 2A). Spontaneous alternation was

FIGURE 2 T-maze spontaneous alternation for WT ($n = 21$), *mdx* ($n = 21$) and *mdx*^{4cv} ($n = 19$) mice. (A) Lower levels of spontaneous alternation were observed in *mdx* and *mdx*^{4cv} compared with WT mice. Chance level is indicated by the dotted line. (B) Alterations per trial did not differ between strains. Asterisks indicate *** $p < 0.001$.

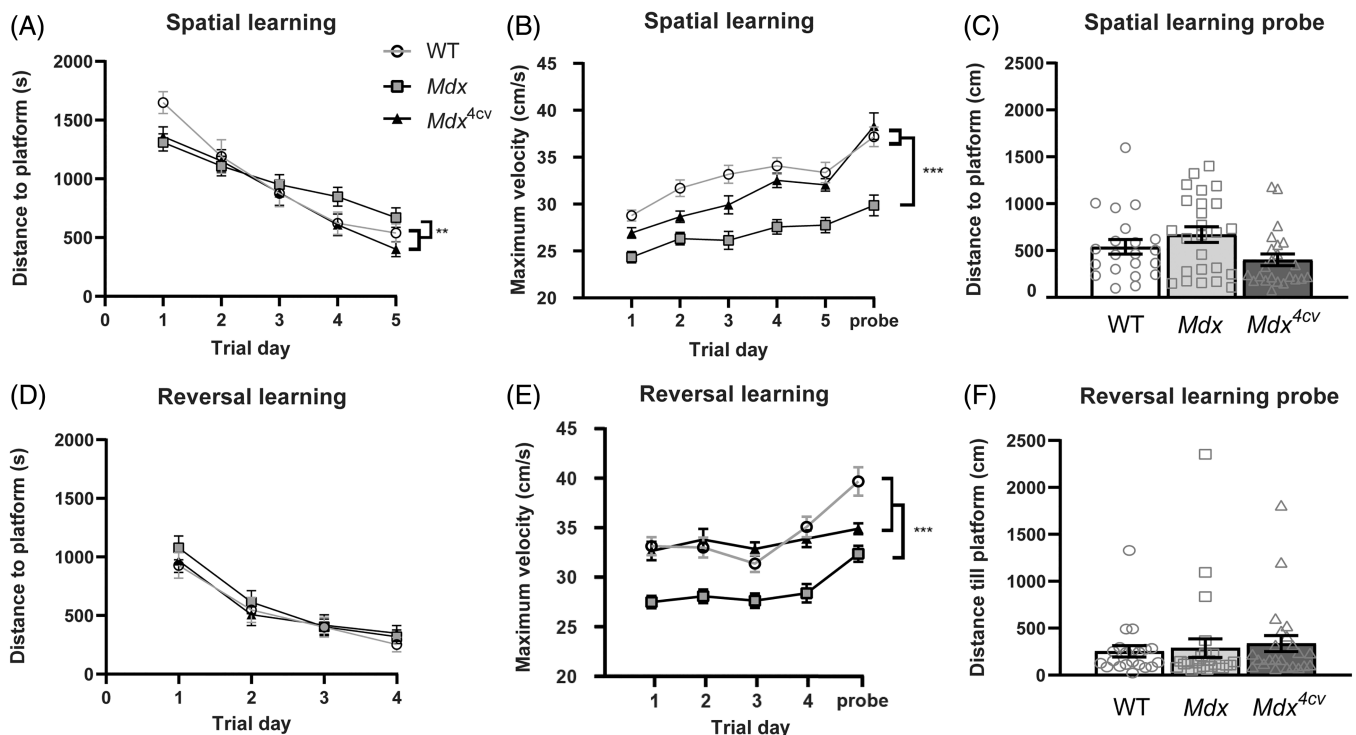
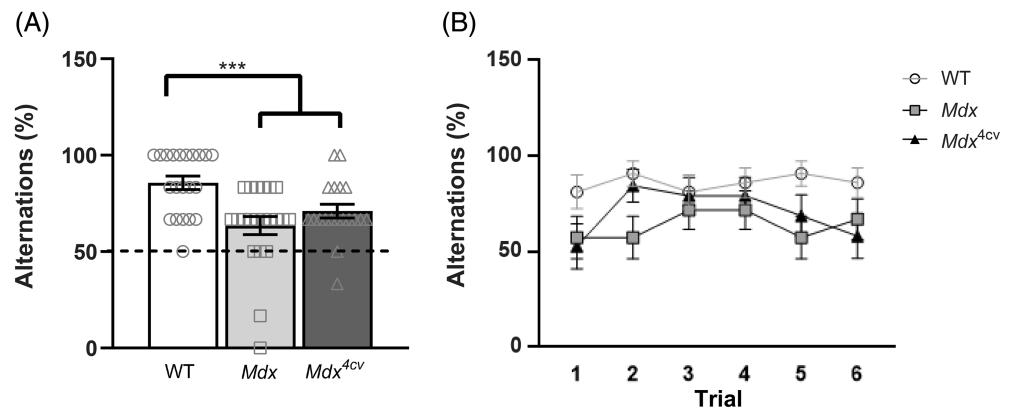


FIGURE 3 Morris water maze spatial and reversal learning for WT ($n = 21$), *mdx* ($n = 25$) and *mdx*^{4cv} ($n = 23$) mice. (A) Distance to platform average of all trials per day. All mice had the capacity to learn the platform location as indicated by the decrease in average distance required to locate the platform. *Mdx* mice had a decreased learning speed compared with WT and *mdx*^{4cv} mice. (B) Maximum swim velocity was significantly lower in *mdx* compared with WT and *mdx*^{4cv} mice. (C) Average distance swam to reach the platform zone during the probe trial. (D) Distance to platform average of all trials per day. All mice had a comparable capacity to learn the new platform location as indicated by the decrease in average distance swam to the platform. (E) Maximum swim velocity was significantly lower in *mdx* compared with WT and *mdx*^{4cv} mice. (F) Average distance swam to reach the platform zone during the probe trial. Asterisks indicate ** $p < 0.01$, *** $p < 0.001$.

defined as entering the previously uninvestigated lateral arm of the T-maze.⁴⁰

Both *mdx* and *mdx*^{4cv} mice showed lower levels of spontaneous alternation compared with WT ($p < 0.001$ and $p = 0.007$, respectively). However, spontaneous alternation was still above chance level of 50% in *mdx* ($p = 0.017$) and *mdx*^{4cv} ($p < 0.001$) mice, suggesting that their spatial working memory was not fully impaired. Mice performance did not differ significantly between different trials, suggesting a minimal effect of repeated exposure (Figure 2B).

3.2 | Delay in spatial learning only visible in *mdx* mice in Morris water maze

As Dp140 is thought to play a role in synaptic plasticity, which is a key player in mechanisms underlying learning and memory, we hypothesized that lack of Dp140 could negatively affect learning capabilities for both forward and reversal learning. The MWM was used to assess spatial reference memory. During acquisition, all strains showed the ability to learn the location of the platform

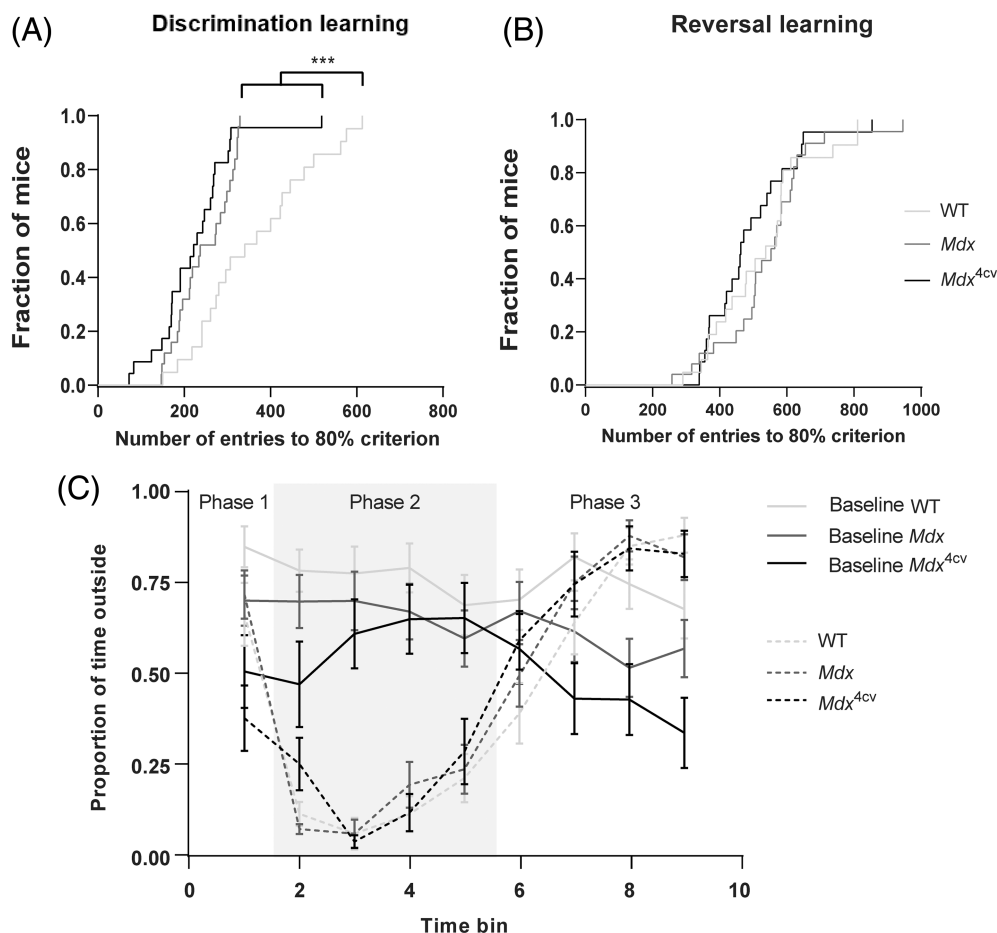


FIGURE 4 Discrimination- and reversal learning with cognition wall and anxiety in PhenoTyper cages for WT ($n = 21$), *mdx* ($n = 23$ – 25) and *mdx*^{4cv} ($n = 22$ – 23) mice. 80% success rate was calculated over a time window of 30 entries. (A) Survival curve of discrimination learning trials. *Mdx* and *mdx*^{4cv} mice were significantly faster in reaching the 80% criterium than WT during discrimination learning. (B) Survival curves of reversal learning trials. No differences were found between groups. (C). Grey area (phase 2) represents the time the light was on. All groups showed a significant response to the light in phase 2 compared with baseline measurements of 24 h earlier. No differences were found between groups in the anxiety response. Asterisks indicate *** $p < 0.001$.

as indicated by a significant effect of trial day on the distance to reach the platform ($p < 0.001$). *Mdx* mice had a lower learning speed compared with WT ($p = 0.002$) and *mdx*^{4cv} mice ($p = 0.003$) (Figure 3A). Learning was measured in terms of distance swam instead of latency, due to the differences found in swimming velocity, to minimize the influence of muscle functionality on the task outcomes. Interestingly, only *mdx* mice showed lower maximum swimming velocity when compared with both WT and *mdx*^{4cv} mice (both $p < 0.001$) (Figure 3B). During the probe test, in which the platform was removed, no differences were found between groups for distance swam to reach the platform zone (Figure 3C).

Unlike forward learning, reversal learning requires the animals to be flexible and adjust their previous learned knowledge and behavior.⁴¹ By changing the conditions of the earlier established task, cognitive flexibility was assessed. During these reversal learning trials, in which mice had to find the new platform location, no differences were found in the distance traveled to reach the platform (Figure 3D). Also here, maximum swimming velocity was significantly lower in *mdx* compared with WT mice and *mdx*^{4cv} (both $p < 0.001$) (Figure 3E). During the reversal probe, no significant differences were observed in distance swam to reach the platform zone (Figure 3F).

3.3 | DMD mice outperform WT in food rewarded discrimination, but not in reversal learning

To further assess different aspects of memory, the PhenoTyper cages were used to perform a food driven discrimination and reversal learning task. The amount of entries needed to reach an 80% success rate was calculated per mouse on a 30 entry window for both discrimination-, and reversal learning trials. Survival curves were calculated and compared between groups (Figure 4A,B). During discrimination learning, *mdx* ($p = 0.032$) and *mdx*^{4cv} ($p = 0.006$) mice reached the 80% criterium faster than WT. No significant differences were found during the reversal learning in the amount of entries or neutral and perseverative errors (data not shown).

3.4 | No differences in light induced anxiety related behavior in DMD mouse models

During the third night in the PhenoTyper cages, a bright light was illuminated to assess the anxiety reaction in the mice. Time spent outside the shelter was measured in 15 min bins starting 15 min before the light went on (phase 1), during the light exposure (phase 2) and for 1 h after the light was turned off (phase 3). Measurements were

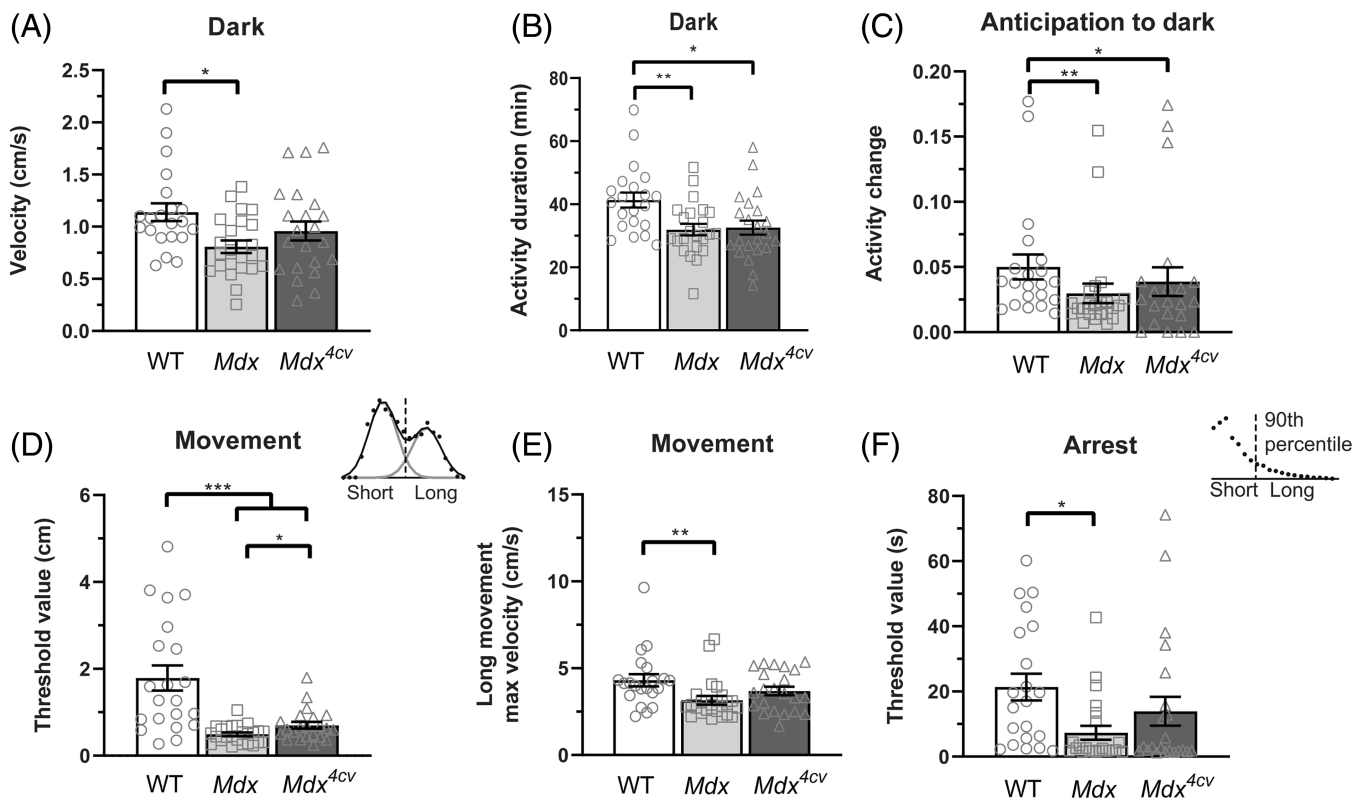


FIGURE 5 Spontaneous behavior in PhenoTyper cages for WT ($n = 21$), *mdx* ($n = 23$) and *mdx*^{4cv} ($n = 22$) mice. (A) Average velocity was lower in *mdx* mice compared with WT mice during the dark phase. (B) The duration of active behavior was shorter in both DMD models compared with WT mice in the dark phase. (C) *Mdx* and *mdx*^{4cv} mice showed a smaller change in activity in anticipation of the start of the dark phase, compared with WT mice. (D) Long movement threshold values revealed decreases in threshold for both *mdx* and *mdx*^{4cv} mice compared with WT mice (E) Maximum velocity of long movement segment was decreased in *mdx* compared with WT mice. (F) Long movement arrest threshold was significantly lower in *mdx* mice compared with WT mice. Asterisks indicate * $p < 0.05$, ** $p < 0.01$, *** $p < 0.001$. Cartoons are taken from Loos et al. 2014.

compared with baseline levels of the strain 24 h earlier. All groups reacted to the light stimulus with decreased time spent outside the shelter (WT: $p < 0.001$, *mdx*: $p < 0.001$ and *mdx*^{4cv}: $p = 0.002$), but no differences were found between groups (Figure 4c) due to the plateau reaction in WT mice.

3.5 | Activity and movement related parameters of spontaneous behavior are affected in both DMD models

To assess different aspects of spontaneous behavior such as activity, changes before and during light switches and movement and arrest patterns, 20 parameters were assessed as described by Loos et al.³³ (Table S3). To determine the possible influence of decreased muscle functionality on spontaneous behavior, the average walking velocity was assessed during the 2nd light and dark phase in the PhenoTyper cages (Figure 5A). *Mdx* mice, but not *mdx*^{4cv} mice, had decreased walking velocity in the dark phase compared with WT mice ($p = 0.012$). Overall activity patterns were furthermore affected in the DMD mouse models (Figure 5B,C). During the dark phase overall activity

was lower in both *mdx* ($p = 0.008$) and *mdx*^{4cv} mice ($p = 0.015$) compared with WT mice (Figure 5B). Additionally, the extent to which overall activity was changed during the last 2 h of the light phase (anticipation of the dark phase) was lower in both *mdx* and *mdx*^{4cv} mice compared with WT mice ($p = 0.001$ and $p = 0.041$, respectively) (Figure 5C).

Movement and arrest segments were identified and duration and distance traveled were determined for each segment. Frequency plots were made for the distance traveled during each movement. On these plots, 2 Gaussian curves were fitted and thresholds were determined by the intersection of the two curves, as described in Loos et al.³³ (Figure 5D-F). Both *mdx* and *mdx*^{4cv} mice showed decreased long movement threshold values compared with WT ($p < 0.001$ for both) (Figure 5D). Furthermore, *mdx* mice showed a lower maximum velocity in the long movement segments compared with WT mice ($p = 0.007$) (Figure 5E). For the duration of each arrest, only one Gaussian curve was fitted and the threshold was determined by calculating the 90th percentile of the area under the fitted curve. This threshold, to separate short and long arrest segments, was reduced in *mdx* mice compared with WT mice ($p = 0.021$) (Figure 5F). Altogether these changes indicate an altered movement pattern being most prominently in *mdx* mice.

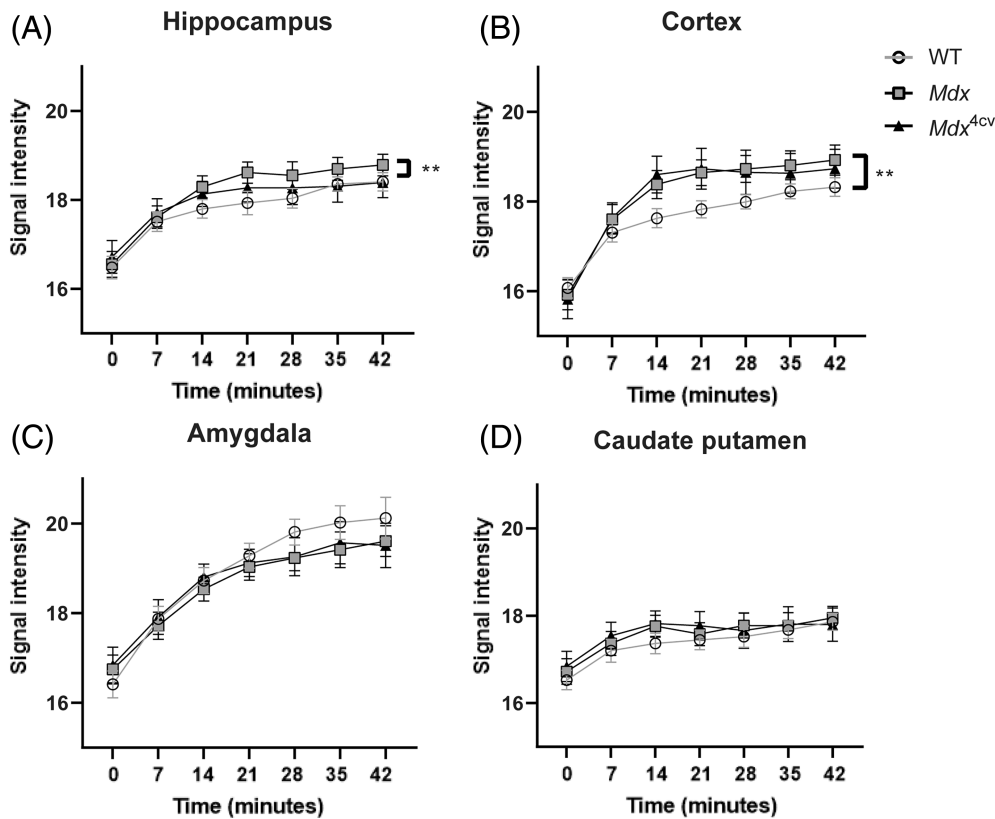


FIGURE 6 Blood-brain barrier permeability in WT ($n = 10$), *mdx* ($n = 9$) and *mdx*^{4cv} ($n = 10$) mice. (A) Signal intensity of the hippocampus. *Mdx* mice had increased T1 values compared with WT. (B) Signal intensity of the cortex. *Mdx*^{4cv} mice showed increased T1 values compared with WT. (C) Signal intensity of the amygdala. (D) Signal intensity of the caudate putamen. Asterisks indicate $**p < 0.01$.

3.6 | Decreased blood-brain barrier integrity in the hippocampus and cortex in DMD mouse models

The blood-brain barrier (BBB) is an important structure in the brain and its integrity is known to be affected in *mdx* mice.⁴² To determine if BBB alterations are similar between DMD models, BBB permeability was analyzed by in vivo MRI. Prior to sacrifice, in vivo MRI was used to image brain structure and to assess BBB integrity. Additionally, volumes of the total brain and 23 specific regions were assessed and compared between the strains. No differences in volume were found in any of the brain regions between strains (Table S4).

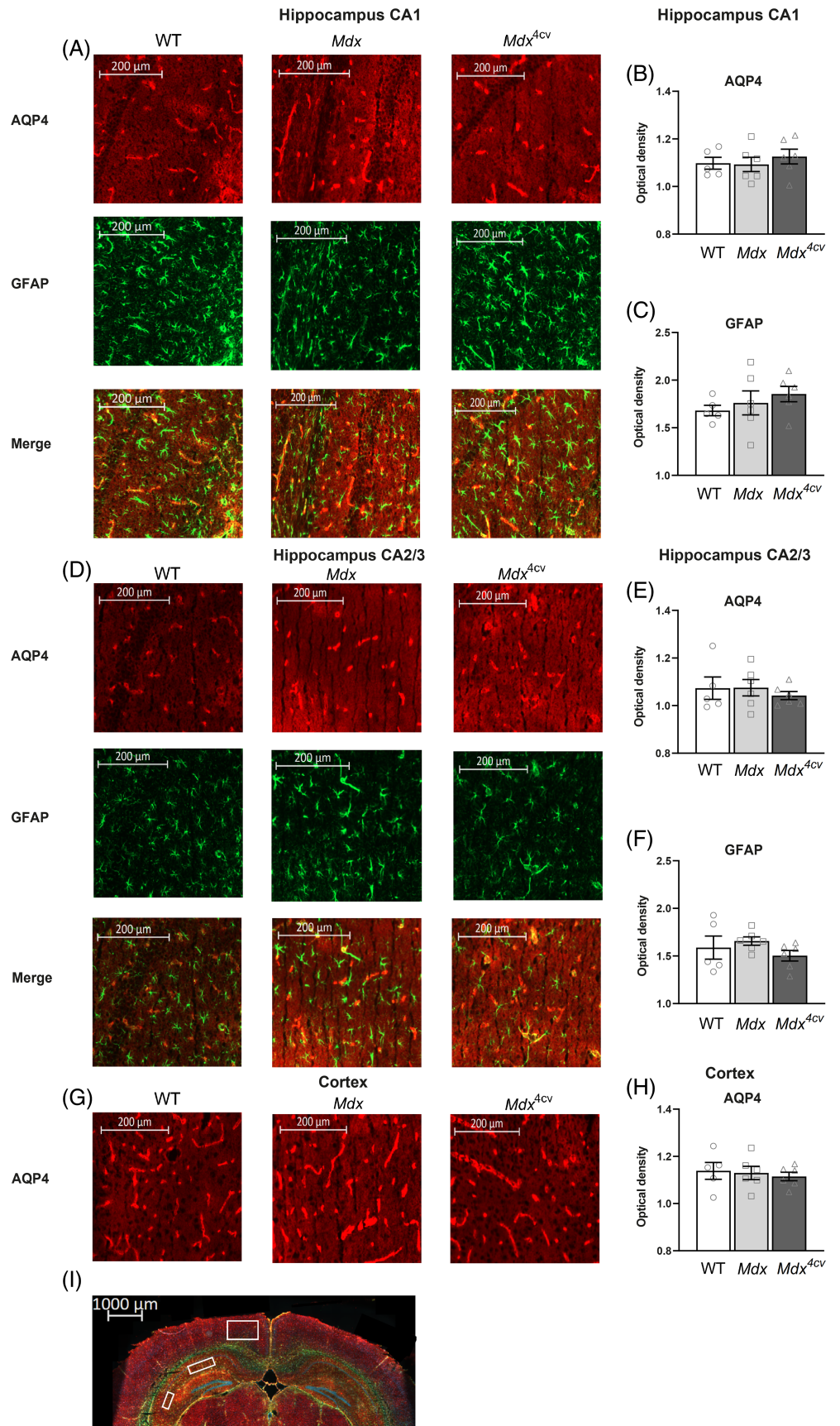
To determine the BBB integrity, mice were scanned at baseline and at six subsequent 1 min intervals after intraperitoneal injection of the contrast solution gadoteridol. One *mdx* mouse was excluded from the analysis due to abnormally high values (>2 STDs higher than average) in multiple regions. Linear mixed models were used to assess the influence of mouse strains on timelapses for BBB integrity for the hippocampus, cortex, amygdala and caudate putamen, as these areas have high dystrophin expression levels in WT mice (Figure 6). *Mdx* mice showed increased BBB permeability in the hippocampus ($p = 0.007$) and in the cortex ($p = 0.058$), reaching only significance in the hippocampus (Figure 6A,B). *Mdx*^{4cv} mice had increased permeability in the cortex compared with WT mice ($p = 0.007$), but not in the hippocampus. Permeability in the amygdala was lower in both DMD strains compared with WT, but this did not reach significance ($p = 0.058$) (Figure 6C). No differences were found in permeability in the caudate putamen (Figure 6D).

To confirm MRI observations, immune-fluorescence stainings for aquaporin 4 (AQP4), a channel that enhances water flux in the brain, and glial fibrillary acidic protein (GFAP), a hippocampal astrocyte marker, were done on cryosections of 6 mice per group. Overall expression intensity was determined in hippocampus CA1 and CA3 regions for both AQP4 and GFAP, and in the cortex for AQP4, however no differences were found in any of the regions (Figure 7). One WT mouse had to be excluded due to freezing damage of the brain slides.

4 | DISCUSSION

The consequences of a lack of full-length dystrophin on the brain in *mdx* mice have been investigated by numerous studies. They provided us with a wide variety of affected cognitive processes, including learning and memory, but research focusing on the consequences of cumulative loss of distinct dystrophin isoforms in the brain is sparse. This study aimed to unravel these consequences on cognition and brain pathology, focusing on spontaneous behavior, different types of learning and memory, anxiety and blood-brain barrier pathology. Some of the tests conducted are known to show only mild deficits in *mdx* mice, but they were deliberately selected to allow detection of potential additional effects induced by the lack of Dp140. Using behavioral paradigms and brain analyses previously unexplored in mice lacking Dp140, we showed similar behavior and pathology for *mdx* and *mdx*^{4cv} mice, indicating minimal involvement

FIGURE 7 Immunohistochemical staining quantification of AQP4 and GFAP in WT ($n = 5$), *mdx* ($n = 6$) and *mdx*^{4cv} ($n = 6$) mice. (A) Representative images of AQP4 and GFAP expression in the CA1 region of the hippocampus of a WT, *mdx* and *mdx*^{4cv} mouse. (B) No significant differences in expression levels of AQP4 in the CA1 region of the hippocampus. (C) No significant differences in expression levels of GFAP in the CA1 region of the hippocampus. (D) Representative images of AQP4 and GFAP expression in the CA2/3 region of the hippocampus of a WT, *mdx* and *mdx*^{4cv} mouse. (E) No significant differences in expression levels of AQP4 in the CA2/3 region of the hippocampus. (F) No significant differences in expression levels of GFAP in the CA2/3 region of the hippocampus. (G) Representative images of AQP4 expression in the cortex of a WT, *mdx* and *mdx*^{4cv} mouse. (H) No significant differences in expression levels of AQP4 in the cortex. (I) Representative image of a WT mouse, showing the location of the ROIs drawn for each region.



of Dp140 in processes of spontaneous behavior and different aspects of learning and memory.

Both *mdx* and *mdx*^{4cv} showed decreased alternations in the T-maze, which contradicts with the study of Rummelink et al that used a different protocol in which mice were forced forward with a protruding latch.⁴³ The decrease in alternation in our current study could indicate a partial deficit in working memory, however other factors, such as anxiety, could have influenced the alternation patterns. *Mdx* mice, and mice lacking Dp140 in addition, have increased anxiety,^{23,26,28,43} which could have led to a preference for the previously explored areas. However, performance was consistent between trials, suggesting minimal involvement of habituation or stress due to repeated exposure. It should be noted that we did not find increased anxiety in our study using the light bulb test in the PhenoTyper cages, however since WT mice drastically minimized their exposure to the stimulus during this test, it was almost impossible to reach even lower levels for the DMD models. Therefore, the lack of difference in anxiety in our study is most likely due to a suboptimal methodology, in which the lux of the lamp was probably too high, and does not directly contradict earlier research on increased anxiety in mice lacking Dp427 and Dp140.²⁸

During the spatial learning phase in the MWM test, *mdx* mice showed a decreased learning curve, indicating a delay, but not a total deficit in spatial learning. They also experienced more difficulty with swimming, as indicated by their decreased velocity, and thus stress which could have affected their learning potential. Previous studies, using a similar protocol, however, failed to show this delay in spatial learning in *mdx* mice even though they did observe lower swimming velocity.^{22,44} It remains unclear why the decreased spatial learning was not observed in *mdx*^{4cv} mice. The MWM test is heavily reliant on muscle performance, and even though we tried to compensate for this by excluding parameters related to swim speed, like latency, we cannot rule out that stress or fatigue has influenced the results. Therefore, it would be beneficial to further investigate spatial learning and memory in a less demanding task in terms of motor function.

In contrast to the decreased performance in working and spatial memory, *mdx* and *mdx*^{4cv} mice outperformed WTs in a food rewarded discrimination learning task, which we had not observed in earlier studies.^{43,45} Increased performance in food motivated tasks has been observed in *mdx* mice before.⁴⁶ This likely results from an increased food drive derived from their skeletal muscle hypertrophy induced increased metabolic demand. Interestingly, this did not affect learning capacity during the reversal learning test. It could be argued that the lack of outperformance of WTs would be counterbalanced by a learning flexibility delay in *mdx* mice. However, lack of evidence on deficits in reversal learning in *mdx* mice in the MWM, makes this hypothesis unlikely. Deficits in fear-learning, which is heavily dependent on the amygdala⁴⁷ have been studied before in *mdx* and *mdx52* mice, lacking Dp427 and Dp140.²⁸ Spatial learning and spontaneous alterations are less dependent on amygdala involvement, but more on the hippocampus.^{48,49} This suggests that learning and memory deficits caused by the lack of Dp140 are mostly dependent on the amygdala.

Spontaneous behavior was assessed in the PhenoTyper cages, using 24 h automated tracking. All parameters were subtracted from the exact same time windows during the day to minimize influences of circadian rhythm on muscle performance.^{50,51} Spontaneous activity of *mdx* and *mdx*^{4cv} mice was mostly altered in terms of movement and arrest patterns and activity, which are heavily influenced by muscle function. Interestingly, this effect seemed more pronounced in *mdx* mice, while literature has shown that the additional lack of Dp140 could further exacerbate motor function.⁵² However, it should be noted that the difference between *mdx* and *mdx*^{4cv} mice was minimal. Since other aspects of spontaneous behavior, like sheltering behavior and habituation, were unaffected, the differences in movement and activity are most likely secondary to muscle fatigue and do not directly point to CNS involvement. However, these results do stress the importance of awareness of muscles involvement in behavioral experiments.

BBB permeability was increased in both *mdx* and *mdx*^{4cv} mice, however not in the same manner. While *mdx* mice showed decreases in BBB integrity in the hippocampus and a trend in the cortex, only the cortex was affected in *mdx*^{4cv} mice. Even though BBB permeability has not been studied before in this manner in *mdx* mice, it is known that the structure and the development of the BBB is affected in these mice and that mice suffer from abnormal cerebral diffusion and perfusion.⁵³ Literature has shown alterations in expressions of multiple proteins associated with BBB integrity or development, including a reduction of AQP4 and GFAP.^{42,54-56} Interestingly, we could not detect decreases in AQP4 nor GFAP levels in our study. Confirmation of immunohistochemical results by other types of protein quantifications would be desired, however lack of tissue samples prohibits further investigations. Furthermore, the age of the mice could influence the inconsistencies between our study and literature and deviations in AQP4 or GFAP expression at other time points cannot be ruled out. It should be noted that Dp71, a shorter dystrophin isoform that is still present in both *mdx* and *mdx*^{4cv} mice is known to interact with AQP4 clustering. While AQP4 does not seem to be the main player in BBB permeability in our study, it could be affected and influencing cognition in DMD models lacking the shorter dystrophin isoforms. Nevertheless, we showed that lack of Dp427 can affect the functioning of the BBB, resulting in increased permeability in multiple regions, while Dp140 does not seem to have an added effect on BBB permeability in our model. While both *mdx* and *mdx*^{4cv} mice lack different dystrophin isoforms, the expression of Dp71 and Dp40 remains unaffected. It is known that DMD patients with mutations affecting these shorter isoforms suffer from more severe behavioral and cognitive deficits.^{8,20} It would be of interest to investigate the additional effects of the loss of Dp71 and Dp40 in mice in the future.

5 | CONCLUSION

Overall we confirmed earlier research in *mdx* mice showing partial deficits in different learning domains and showed that they do not have CNS related deviations in spontaneous behavior. Lack of Dp140

is known to increase anxiety and cause deficits in fear learning. However the additional lack of Dp140 in *mdx^{Acv}* mice did not lead to substantial differences compared with *mdx* mice in any of our tests, indicating a minimal or no role of Dp140 in tasks related to different types of hippocampal dependent memory or spontaneous behavior. Whether Dp140 plays a role in other cognitive processes has yet to be determined.

AUTHOR CONTRIBUTIONS

M. Verhaeg: Investigation; software; formal analysis; writing-original draft; writing-review & editing; visualization. **K. Adamzek:** Methodology; investigation. **D. van de Vijver:** Investigation. **K. Putker:** Investigation. **S. Engelbeen:** Investigation. **D. Wijnbergen:** Software. **M. Overzier:** Investigation. **E. Suidgeest:** Investigation. **L. van der Weerd:** Supervision; validation. **A. Aartsma-Rus:** Conceptualization; validation; resources; writing- review & editing; supervision; project administration. **M. van Putten:** Conceptualization; methodology; writing- review & editing; supervision; funding acquisition.

ACKNOWLEDGMENTS

We would like to acknowledge Max Gentenaar for his help with the histology and Pietro Spitali for generating a data analysis script.

FUNDING INFORMATION

This project was funded by Duchenne Parent Project-NL and Duchenne Parent Project Belgium grant 15.003.

CONFLICT OF INTEREST STATEMENT

None related to this work. For full transparency, AAR discloses being employed by LUMC, which has patents on exon skipping technology, some of which has been licensed to BioMarin and subsequently sublicensed to Sarepta. As co-inventor of some of these patents AAR is entitled to a share of royalties. AAR further discloses being ad hoc consultant for PTC Therapeutics, Sarepta Therapeutics, Regenxbio, Alpha Anomeric, Lilly BioMarin Pharmaceuticals Inc., Eisai, Entrada, Takeda, Splicesense, Galapagos, MitoRx and Astra Zeneca. Past ad hoc consulting has occurred for: CRISPR Therapeutics, Summit PLC, Audentes Santhera, Bridge Bio, Global Guidepoint and GLG consultancy, Grunenthal, Wave and BioClinica. AAR also reports having been a member of the Duchenne Network Steering Committee (BioMarin) and being a member of the scientific advisory boards of Eisai, hybridize therapeutics, silence therapeutics, Sarepta therapeutics. Past SAB memberships: ProQR, Philae Pharmaceuticals. Remuneration for these activities is paid to LUMC. LUMC also received speaker honoraria from PTC Therapeutics, Alnylam Netherlands, Pfizer and BioMarin Pharmaceuticals and funding for contract research from Italfarmaco, Sapreme, Eisai, Galapagos, Synnaffix and Alpha Anomeric. Project funding is received from Sarepta Therapeutics and Entrada.

DATA AVAILABILITY STATEMENT

The data that support the findings of this study are available from the corresponding author upon request.

ETHICS STATEMENT

The animal study was reviewed and approved by Central Authority for Scientific Procedures on Animals and performed according to Dutch regulation for animal experimentation, and in accordance with EU Directive 2010/63/EU.

ORCID

Minou Verhaeg  <https://orcid.org/0000-0001-9142-0972>

Maike van Putten  <https://orcid.org/0000-0002-0683-8897>

REFERENCES

- Aartsma-Rus A, Ginjaar IB, Bushby K. The importance of genetic diagnosis for Duchenne muscular dystrophy. *J Med Genet.* 2016;53:145-151.
- Emery AE. The muscular dystrophies. *Lancet.* 2002;359:687-695.
- Banihani R, Smile S, Yoon G, et al. Cognitive and neurobehavioral profile in boys with Duchenne muscular dystrophy. *J Child Neurol.* 2015;30:1472-1482.
- Hinton V, Fee R, Goldstein E, de Vivo D. Verbal and memory skills in males with Duchenne muscular dystrophy. *Dev Med Child Neurol.* 2007;49:123-128.
- Billard C, Gillet P, Signoret J, et al. Cognitive functions in Duchenne muscular dystrophy: a reappraisal and comparison with spinal muscular atrophy. *Neuromuscul Disord.* 1992;2:371-378.
- Hendriksen JG, Vles JS. Neuropsychiatric disorders in males with duchenne muscular dystrophy: frequency rate of attention-deficit hyperactivity disorder (ADHD), autism spectrum disorder, and obsessive-compulsive disorder. *J Child Neurol.* 2008;23:477-481.
- Hinton VJ, Nereo NE, Fee RJ, Cyrulnik SE. Social behavior problems in boys with Duchenne muscular dystrophy. *J Dev Behav Pediatr.* 2006;27:470-476.
- Ricotti V, Mandy WP, Scoto M, et al. Neurodevelopmental, emotional, and behavioural problems in Duchenne muscular dystrophy in relation to underlying dystrophin gene mutations. *Dev Med Child Neurol.* 2016;58:77-84.
- Waite A, Brown SC, Blake DJ. The dystrophin-glycoprotein complex in brain development and disease. *Trends Neurosci.* 2012;35:487-496.
- Lidov HG, Byers TJ, Watkins SC, Kunkel LM. Localization of dystrophin to postsynaptic regions of central nervous system cortical neurons. *Nature.* 1990;348:725-728.
- Nudel U, Zuk D, Einat P, et al. Duchenne muscular dystrophy gene product is not identical in muscle and brain. *Nature.* 1989;337:76-78.
- Holder E, Maeda M, Bies RD. Expression and regulation of the dystrophin Purkinje promoter in human skeletal muscle, heart, and brain. *Hum Genet.* 1996;97:232-239.
- Doorenweerd N, Mahfouz A, van Putten M, et al. Timing and localization of human dystrophin isoform expression provide insights into the cognitive phenotype of Duchenne muscular dystrophy. *Sci Rep.* 2017;7:12575.
- Blake DJ, Kröger S. The neurobiology of Duchenne muscular dystrophy: learning lessons from muscle? *Trends Neurosci.* 2000;23:92-99.
- Hashimoto Y, Kuniishi H, Sakai K, et al. Brain Dp140 alters glutamatergic transmission and social behaviour in the *mdx52* mouse model of Duchenne muscular dystrophy. *Prog Neurobiol.* 2022;216:102288.
- Anderson JL, Head SI, Morley JW. Duchenne muscular dystrophy and brain function. In: Hedge M, Ankala A, eds. *Muscular Dystrophy Intech.* Intech; 2012:91-122.
- Daoud F, Angeard N, Demerre B, et al. Analysis of Dp71 contribution in the severity of mental retardation through comparison of Duchenne and Becker patients differing by mutation consequences on Dp71 expression. *Hum Mol Genet.* 2009;18:3779-3794.

18. Tozawa T, Itoh K, Yaoi T, et al. The shortest isoform of dystrophin (Dp40) interacts with a group of presynaptic proteins to form a presumptive novel complex in the mouse brain. *Mol Neurobiol.* 2012;45:287-297.
19. Chamova T, Guerguelcheva V, Raycheva M, et al. Association between loss of dp140 and cognitive impairment in duchenne and becker dystrophies. *Balkan J Med Genet.* 2013;16:21-29.
20. Taylor PJ, Betts GA, Maroulis S, et al. Dystrophin gene mutation location and the risk of cognitive impairment in Duchenne muscular dystrophy. *PLoS One.* 2010;5:e8803.
21. Miranda R, Nagapin F, Bozon B, Laroche S, Aubin T, Vaillend C. Altered social behavior and ultrasonic communication in the dystrophin-deficient mdx mouse model of Duchenne muscular dystrophy. *Mol Autism.* 2015;6:1-17.
22. Vaillend C, Billard J-M, Laroche S. Impaired long-term spatial and recognition memory and enhanced CA1 hippocampal LTP in the dystrophin-deficient Dmdmdx mouse. *Neurobiol Dis.* 2004;17:10-20.
23. Manning J, Kulbida R, Rai P, et al. Amitriptyline is efficacious in ameliorating muscle inflammation and depressive symptoms in the mdx mouse model of Duchenne muscular dystrophy. *Exp Physiol.* 2014;99:1370-1386.
24. Comim CM, Ventura L, Freiberger V, et al. Neurocognitive impairment in mdx mice. *Mol Neurobiol.* 2019;56:7608-7616.
25. Sekiguchi M, Zushida K, Yoshida M, et al. A deficit of brain dystrophin impairs specific amygdala GABAergic transmission and enhances defensive behaviour in mice. *Brain.* 2009;132:124-135.
26. Vaillend C, Chaussent R. Relationships linking emotional, motor, cognitive and GABAergic dysfunctions in dystrophin-deficient mdx mice. *Hum Mol Genet.* 2017;26:1041-1055.
27. Aupy P, Zarrouki F, Sandro Q, et al. Long-term efficacy of AAV9-U7snRNA-mediated exon 51 skipping in mdx52 mice. *Mol Ther Methods Clin Dev.* 2020;17:1037-1047.
28. Saoudi A, Zarrouki F, Sebr e C, Izabelle C, Goyenville AL, Vaillend C. Emotional behavior and brain anatomy of the mdx52 mouse model of Duchenne muscular dystrophy. *Dis Model Mech.* 2021;14:dmm049028.
29. Zhang C, Li H, Han R. An open-source video tracking system for mouse locomotor activity analysis. *BMC Res Notes.* 2020;13:1-6.
30. Veltrop M, van der Kaa J, Claassens J, VAN Vliet L, Verbeek S, Aartsma-Rus A. Generation of embryonic stem cells and mice for duchenne research. *PLoS Curr.* 2013;5. <https://doi.org/10.1371/currents.md.cbf1d33001de80923ce674302cad7925>
31. Chapman VM, Miller DR, Armstrong D, Caskey CT. Recovery of induced mutations for X chromosome-linked muscular dystrophy in mice. *Proc Natl Acad Sci.* 1989;86:1292-1296.
32. Vorhees CV, Williams MT. Morris water maze: procedures for assessing spatial and related forms of learning and memory. *Nat Protoc.* 2006;1:848-858.
33. Loos M, Koopmans B, Aarts E, et al. Sheltering behavior and locomotor activity in 11 genetically diverse common inbred mouse strains using home-cage monitoring. *PLoS One.* 2014;9:e108563.
34. Aarts E, Maroteaux G, Loos M, et al. The light spot test: measuring anxiety in mice in an automated home-cage environment. *Behav Brain Res.* 2015;294:123-130.
35. Rummelink E, Smit AB, Verhage M, Loos M. Measuring discrimination-and reversal learning in mouse models within 4 days and without prior food deprivation. *Learn Mem.* 2016b;23:660-667.
36. Boehm-Sturm P, F uchtemeier M, Foddiss M, et al. Neuroimaging biomarkers predict brain structural connectivity change in a mouse model of vascular cognitive impairment. *Stroke.* 2017;48:468-475.
37. Huebner NS, Mechling AE, Lee H-L, et al. The connectomics of brain demyelination: functional and structural patterns in the cuprizone mouse model. *Neuroimage.* 2017;146:1-18.
38. Koch S, Mueller S, Foddiss M, et al. Atlas registration for edema-corrected MRI lesion volume in mouse stroke models. *J Cerebral Blood Flow Metab.* 2019;39:313-323.
39. Lein ES, Hawrylycz MJ, Ao N, et al. Genome-wide atlas of gene expression in the adult mouse brain. *Nature.* 2007;445:168-176.
40. Lalonde R. The neurobiological basis of spontaneous alternation. *Neurosci Biobehav Rev.* 2002;26:91-104.
41. Izquierdo A, Brigman JL, Radke AK, Rudebeck PH, Holmes A. The neural basis of reversal learning: an updated perspective. *Neuroscience.* 2017;345:12-26.
42. Nico B, Frigeri A, Nicchia GP, et al. Severe alterations of endothelial and glial cells in the blood-brain barrier of dystrophic mdx mice. *Glia.* 2003;42:235-251.
43. Rummelink E, Aartsma-Rus A, Smit A, et al. Cognitive flexibility deficits in a mouse model for the absence of full-length dystrophin. *Genes Brain Behav.* 2016a;15:558-567.
44. Sesay A, Errington M, Levita L, Bliss T. Spatial learning and hippocampal long-term potentiation are not impaired in mdx mice. *Neurosci Lett.* 1996;211:207-210.
45. Engelbeen S, Aartsma-Rus A, Koopmans B, Loos M, VAN Putten M. Assessment of behavioral characteristics with procedures of minimal human interference in the mdx mouse model for Duchenne muscular dystrophy. *Front Behav Neurosci.* 2021;14:629043.
46. Lewon M, Peters CM, van Ry PM, Burkin DJ, Hunter KW, Hayes LJ. Evaluation of the behavioral characteristics of the mdx mouse model of duchenne muscular dystrophy through operant conditioning procedures. *Behav Processes.* 2017;142:8-20.
47. Phillips R, Ledoux J. Differential contribution of amygdala and hippocampus to cued and contextual fear conditioning. *Behav Neurosci.* 1992;106:274-285.
48. Douglas RJ, Isaacson RL. Hippocampal lesions and activity. *Psychonom Sci.* 1964;1:187-188.
49. Silvers JM, Tokunaga S, Berry RB, White AM, Matthews DB. Impairments in spatial learning and memory: ethanol, allopregnanolone, and the hippocampus. *Brain Res Rev.* 2003;43:275-284.
50. Betts CA, Jagannath A, van Westering TL, et al. Dystrophin involvement in peripheral circadian SRF signalling. *Life Sci Alliance.* 2021;4:e202101014. <https://doi.org/10.26508/lsa.202101014>
51. Gao H, Xiong X, Lin Y, Chatterjee S, Ma K. The clock regulator Bmal1 protects against muscular dystrophy. *Exp Cell Res.* 2020;397:112348.
52. Chesshyre M, Ridout D, Hashimoto Y, et al. Investigating the role of dystrophin isoform deficiency in motor function in Duchenne muscular dystrophy. *J Cachexia Sarcopenia Muscle.* 2022;13:1360-1372.
53. Goodnough CL, Gao Y, Li X, et al. Lack of dystrophin results in abnormal cerebral diffusion and perfusion in vivo. *Neuroimage.* 2014;102:809-816.
54. Frigeri A, Nicchia GP, Nico B, et al. Aquaporin-4 deficiency in skeletal muscle and brain of dystrophic mdx mice. *FASEB J.* 2001;15:90-98.
55. Nicchia G, Nico B, Camassa L, et al. The role of aquaporin-4 in the blood-brain barrier development and integrity: studies in animal and cell culture models. *Neuroscience.* 2004;129:935-944.
56. Vajda Z, Pedersen M, Doczi T, Sulyok E, Nielsen S. Studies of mdx mice. *Neuroscience.* 2004;129:991-996.

SUPPORTING INFORMATION

Additional supporting information can be found online in the Supporting Information section at the end of this article.

How to cite this article: Verhaeg M, Adamzek K, van de Vijver D, et al. Learning, memory and blood-brain barrier pathology in Duchenne muscular dystrophy mice lacking Dp427, or Dp427 and Dp140. *Genes, Brain and Behavior.* 2024;23(3):e12895. doi:[10.1111/gbb.12895](https://doi.org/10.1111/gbb.12895)